

# Extracellular Matrix Assembly in Diatoms (Bacillariophyceae)<sup>1</sup>

## III. Organization of Fucoglucuronogalactans within the Adhesive Stalks of *Achnanthes longipes*

Brandon A. Wustman, Jan Lind, Richard Wetherbee, and Michael R. Gretz\*

Department of Biological Sciences, Michigan Technological University, Houghton, Michigan 49931–1295 (B.A.W., M.R.G.); and School of Botany, University of Melbourne, Parkville, Victoria 3052, Australia (J.L., R.W.)

*Achnanthes longipes* is a marine, biofouling diatom that adheres to surfaces via adhesive polymers extruded during motility or organized into structures called stalks that contain three distinct regions: the pad, shaft, and collar. Four monoclonal antibodies (AL.C1–AL.C4) and antibodies from two uncloned hybridomas (AL.E1 and AL.E2) were raised against the extracellular adhesives of *A. longipes*. Antibodies were screened against a hot-water-insoluble/hot-bicarbonate-soluble-fraction. The hot-water-insoluble/hot-bicarbonate-soluble fraction was fractionated to yield polymers in three size ranges: F<sub>1</sub>, ≥ 20,000,000 M<sub>r</sub>; F<sub>2</sub>, ≈ 100,000 M<sub>r</sub>; and F<sub>3</sub>, < 10,000 M<sub>r</sub> relative to dextran standards. The ≈ 100,000-M<sub>r</sub> fraction consisted of highly sulfated (approximately 11%) fucoglucuronogalactans (FGGs) and low-sulfate (approximately 2%) FGGs, whereas F<sub>1</sub> was composed of O-linked FGG (F<sub>2</sub>)-polypeptide (F<sub>3</sub>) complexes. AL.C1, AL.C2, AL.C4, AL.E1, and AL.E2 recognized carbohydrate complementary regions on FGGs, with antigenicity dependent on fucosyl-containing side chains. AL.C3 was unique in that it had a lower affinity for FGGs and did not label any portion of the shaft. Enzyme-linked immunosorbent assay and immunocytochemistry indicated that low-sulfate FGGs are expelled from pores surrounding the raphe terminus, creating the cylindrical outer layers of the shaft, and that highly sulfated FGGs are extruded from the raphe, forming the central core. Antibody-labeling patterns and other evidence indicated that the shaft central-core region is related to material exuded from the raphe during cell motility.

Because of the complexity of the higher-plant ECM, we have only recently begun to understand the spatial relationships between ECM components, and know little about the intra- and intermolecular interactions responsible for cell wall organization and assembly (Levy and Staehelin, 1992). McCann et al. (1990) succeeded in visualizing the intermolecular organization of the onion primary cell wall, demonstrating cross-links between cellulose and hemicellulose and a separate surrounding network made up pectic polymers. Taylor and Haigler (1993) found that cellulose

serves as a template mediating the self-organization of other molecules such as xylan and Gly-rich proteins in the secondary cell walls of tracheary elements. ECM polymers appear to interact initially through short-range forces, most notably hydrogen bonding. Hydrogen bonding, hydrophobic interactions, and ionic cross-bridging are noncovalent associations essential to maintenance of cell wall integrity. Recently, Ca<sup>2+</sup>-dependent pectin-binding proteins were isolated (Penel and Greppin, 1996), including several vitronectin-like proteins and isoperoxidases. These results indicate that an ion-binding mechanism may be responsible for the organization of some proteins in the plant cell wall. Covalent binding may be a final step in the self-assembly process, cementing together all of the individual components of the matrix. The most common covalent linkages are: (a) sugar-sugar glycosidic linkages; (b) sugar-protein glycosidic linkages; and (c) sugar-sugar, protein-protein, and sugar-protein peroxidase-mediated phenolic cross-links.

The marine, biofouling diatom *Achnanthes longipes* relies on production of highly organized extracellular adhesive biocomposites for cell motility and permanent adhesion to submerged surfaces (Wang et al., 1997; Wustman et al., 1997). The adhesive polymers of *A. longipes* are primarily polysaccharide with a small amount of protein, and preliminary studies suggest the presence of phenolics (Wustman et al., 1997). Extracellular assembly appears to require both cationic cross-bridging and a peroxidase-mediated phenolic cross-linking (Wustman et al., 1997). These extracellular adhesives must be extruded through the silicious cell wall, or frustule, before they can be assembled into permanent attachment structures termed stalks. Because of the relative immutability of the frustule, extrusion of polymers is necessarily limited to openings in the frustule, and protoplasmic mediation of the assembly processes occurring distal to the frustule is restricted. The hydrated, amorphous silica frustule imposes limitations on protoplasm-

<sup>1</sup> This research was supported by the Office of Naval Research (grant nos. N00014-94-1-0273 and N00014-94-1-0766) to M.R.G and Kyle D. Hoagland and a Michigan Technological University Fellowship Award to B.A.W.

\* Corresponding author; e-mail mrgretz@mtu.edu; fax 1-906-487-3167.

Abbreviations: CMC, 1-cyclohexyl-3-(2-morpholinoethyl)carbodiimide-metho-*p*-toluenesulfonate; CPC, cetylpyridinium chloride; ECM, extracellular matrix; FGG, fucoglucuronogalactan; FITC, fluorescein isothiocyanate; TFA, trifluoroacetic acid; WIBS, hot-water-insoluble/hot-bicarbonate-soluble fraction.

mediated control of orientation and on movement of extracellular polymers both during and after synthesis, and on communication across the protoplasm-plasma membrane-extracellular polymer continuum. For this reason, the assembly of complex polysaccharide-protein stalks with a high degree of organization and detailed substructure in diatoms represents a fascinating system in which to study self-assembly phenomena. Moreover, in *A. longipes*, the adhesion process can be easily manipulated with various molecular probes and inhibitors, and extrusion and assembly of the biocomposites can be monitored via time-lapse video microscopy and electron microscopy (Wang et al., 1997). The extracellular adhesive polymers of *A. longipes* have been isolated and purified from cultures in quantities large enough to enable detailed chemical analysis (Wustman et al., 1997), as well as polymer-interaction studies. Thus, the *A. longipes* attachment process represents a unique model system for investigations into cell-substratum adhesion and physical characteristics of extracellular matrices based on polymer composition and polymer-polymer interactions.

The stalks of *A. longipes* can be described as having three distinct regions: a surface-associated pad, a collar associated with the frustule at the raphe terminus, and an intervening shaft that separates the cell from the surface (Daniel et al., 1987; Wang et al., 1997) (Fig. 1A). Transmission electron microscopy, lectin-FITC labeling, and cytochemical staining have demonstrated that the polymers are organized into several outer layers parallel to the axis of shaft elongation, and an inner core oriented in a radial pattern perpendicular to the axis of shaft elongation (Daniel et al., 1987; Wang et al., 1997; Wustman et al., 1997). Distributions of various polymers within the adhesive structure have not been determined, although evidence suggests that covalent cross-linking of polysaccharides by proteins and/or phenolics may be involved (Wustman et al., 1997). We have used lectin-FITC and cytochemical staining in correlation with chemical analysis to identify the presence of certain monosaccharide residues within unique regions of the adhesive structures (Wustman et al., 1997). The initial adhesive found in pads and between stacked cells preparing to separate contained substantial amounts of GlcA and fucosyl residues. Outer layers of the shaft contained GlcA, t-Fuc, and nonsulfated D-Gal residues, whereas the inner core was primarily constituted of sulfated galactosyl residues (Johnson, 1995; Wustman et al., 1997).

Puhlmann et al. (1994) generated monoclonal antibodies to several cell wall components of suspension-cultured sycamore maple cells, and Freshour et al. (1996) used them to help discern the pattern of organization within the ECM and to determine how these patterns changed during different stages of root development in *Arabidopsis thaliana* seedlings. ECM assembly and physical characteristics can also be investigated by discerning which epitopes are directly involved in polymer-polymer or polymer-surface interactions. We report here the characterization of several monoclonal antibodies generated against extracellular adhesives of *A. longipes*. Based in part on the affinities and labeling patterns of these antibodies, we have created a model that predicts how polymers are organized into su-

pramolecular complexes (adhesive stalks) by *A. longipes* and identifies chemically unique regions within the stalk substructure. Based on these results, we can begin to correlate polymer structure and polymer interactions with the overall physical characteristics of the extracellular adhesive.

## MATERIALS AND METHODS

### Source of Algal Material, Culturing Conditions, and Chemical Isolation of Diatom ECM

*Achnanthes longipes* Ag. (no. 330), *Amphora coffeaeformis* Ag. Kütz. (no. 2080), and *Cymbella cistula* (Ehr.) Kirchn. were obtained and cultured as described by Wustman et al. (1997). *Stauroneis decipiens* was isolated and cultured as described by Lind et al. (1997). WIBS, WIBS/CPC-soluble ECM fractions of *A. longipes* and *A. coffeaeformis*, and WIBS/CPC-insoluble ECM fractions of *A. longipes* and *A. coffeaeformis* were isolated as described by Wustman et al. (1997).

### Generation of Hybridoma Cell Lines

*A. longipes* cells and ECM were scraped from 3-week-old culture flasks and fixed with 2% glutaraldehyde. Fixed cells and ECM (2 mg) were mixed with an equal amount of methylated BSA in PBS (20 mM PO<sub>4</sub>, 0.15 M NaCl, pH 7.2), an equal volume of Titremax adjuvant (CytRx, Norcross, GA) was added, and 200  $\mu$ L was injected (intraperitoneally) into female Balb/c mice. A second injection of 200  $\mu$ L was administered 1 month after the first, and a final 200- $\mu$ L boost, consisting of *A. longipes* WIBS material mixed with an equal volume of methylated BSA in PBS without adjuvant, was injected 2 d before fusion.

Spleenocytes were fused with the X63Ag.653 myeloma cell line and hybridomas were grown as described by Harlow and Lane (1988). Hybridoma supernatant was screened by ELISA against *A. longipes* WIBS material with detection of bound antibodies by anti-mouse whole IgG conjugated to alkaline phosphatase (Sigma) and by antibody-FITC cell staining of unfixed cells as described below. During the screening process we selected against hybridomas producing antibodies that bound to bacteria. Positive cell lines were cloned by limiting dilution.

### Isotyping of Monoclonal Antibodies

Isotyping of monoclonal antibodies and antibodies from uncloned, extended hybridoma cell lines was done using the Amersham Mouse Monoclonal Antibody Isotyping Kit (RPN 29, Amersham).

### ELISA

*A. longipes* WIBS material was dissolved in PBS (20 mM PO<sub>4</sub>, 0.15 M NaCl, pH 7.2) (50  $\mu$ g/mL) and incubated in microtiter trays (Probind Falcon, Becton Dickinson) at 37°C for 1 h. Wells were washed twice with PBS containing 1% (w/v) BSA, incubated at 37°C for 1 h with PBS containing 1% (w/v) BSA, and washed once with PBS. Hybridoma

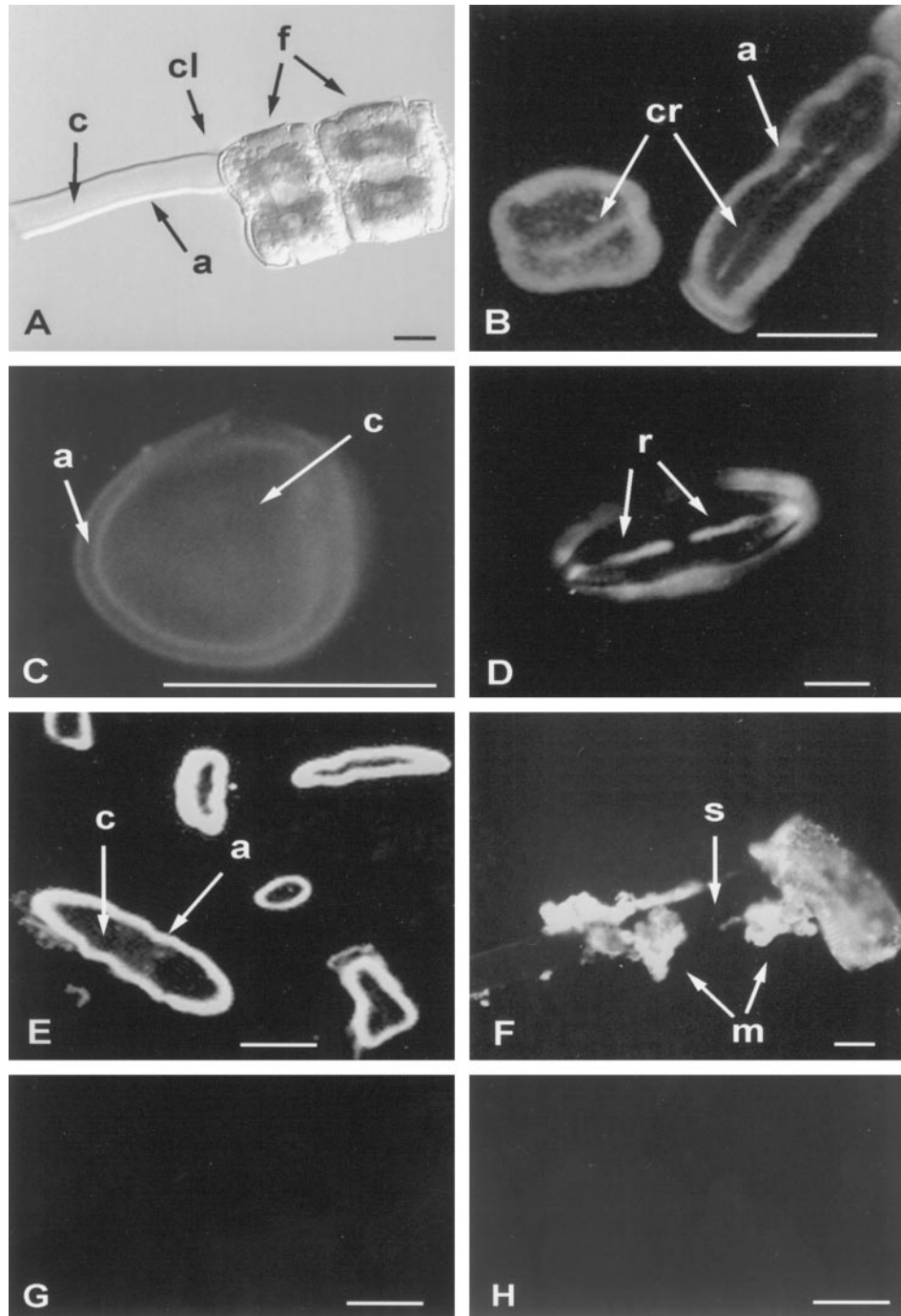


**Figure 1.** *A. longipes* ECM and antibody localization. A, Differential interference contrast microscopy image of *A. longipes* showing the frustules (f), collar (cl), outer shaft regions (a), and inner shaft core (c). B through H, Fluorescent antibody labeling (B, C, E, G, and H on 200-nm sections): B, AL.E1 localization of the outer shaft region and central ribbon (cr) of the shaft core; C, AL.C1 labeling of the inner shaft core; D, AL.C1 labeling of the raphe region of a cell (r) and material associated with the frustule; E, AL.E2 localization of the outer shaft regions; F, AL.C3 localization of globular matrix material (m) associated with the shaft (s). G, Sections incubated with preimmune serum in place of hybridoma supernatant. H, Sections incubated with ascites fluid in place of hybridoma supernatant. The same photographic exposure times were used to image controls and sections incubated with the hybridoma supernatant. Scale bars = 5  $\mu\text{m}$ .

supernatant or mouse serum (diluted 1:500 in PBS) was incubated at 37°C for 1 h and washed five times with PBS containing 0.5% Tween 20 (v/v). Antibody binding was

detected by a secondary antibody (goat anti-mouse IgG, IgM, or polyvalent immunoglobulin labeled with FITC, diluted 1:1000 in PBS with 4% [w/v] PEG, 0.5% [v/v]

Tween 20, and 1% [w/v] ovalbumin). The wells were incubated with secondary antibody for 1 h at 37°C, washed four times with PBS containing 0.5% (v/v) Tween 20, and two times with double-distilled water. One hundred microliters of phosphate substrate solution (1 mg/mL *p*-nitrophenylphosphate in 10 mM diethanolamine, 0.5 M MgCl<sub>2</sub>, pH 9.5) was added to each well and incubated for 20 min at 24°C, and the A<sub>405</sub> was read.

### Antibody-FITC Cell Staining

Diatom cells and ECM were isolated from culture, washed in microcentrifuge tubes with marine PBS (20 mM PO<sub>4</sub>, 0.5 M NaCl, pH 7.2) for 10 min, followed by a stepwise marine PBS:PBS gradient (3:1, 1:1, 1:3, 100% PBS, 5 min/wash), and incubated for 30 min with 0.05% (w/v) Gly and for 1 h in FGB-PBS (PBS containing 1% [v/v] fish skin gelatin and 0.02% [v/v] Tween 20). Cells were centrifuged at 500g for 2 min, the supernatant was discarded, and the pellet was resuspended in mouse serum or hybridoma supernatant (diluted 1:25 in FGB-PBS). After incubation for 3 h at 24°C, cells were washed four times with FGB-PBS (5 min each), resuspended in 10 μL of secondary antibody (goat anti-mouse IgG, IgM, or polyvalent immunoglobulins [IgG, IgA, IgM] labeled with FITC, diluted 1:25 in FGB-PBS), incubated at 24°C for 1 h in the dark, and washed five times with FGB-PBS. The cells were resuspended in 7 μL of *p*-phenylenediamine (1 mg/mL in PBS with 30% [v/v] glycerol) and viewed with differential interference contrast microscopy and epifluorescence microscopy, as described by Wustman et al. (1997). Controls were treated as described above with either preimmune serum or mouse ascites fluid in place of the hybridoma supernatant and by incubating with secondary antibody alone.

For antibody-FITC staining of diatom sections, *A. longipes* cells and associated ECM were fixed and embedded as described by Wang et al. (1997). Sections (200 nm thick) mounted on slides were stained and viewed as described above.

### Column Chromatography

Size-exclusion-gel Sepharose 2B and Sephadex G-100 (Sigma) column dimensions were 20 cm × 1.4 cm and 30 cm × 1.4 cm, respectively. The mobile phase was distilled water or 0.1 or 0.5 M imidazole HCl with a flow rate of 0.8 mL/min. The sample (0.5 mL of 2 mg/mL solution) was loaded onto the columns and the effluent was monitored at 280 nm and collected in 2-mL fractions. Each fraction was screened for carbohydrate using the phenol-sulfuric acid assay, as described below. Identified peaks were collected and screened for antigenicity by dot-blot analysis as described below. Blue dextran 20,000,000 M<sub>r</sub>, dextran 500,000 M<sub>r</sub>, and Glc (Sigma) were used to calibrate the columns.

DEAE-Sephacel anion-exchange support was obtained from Sigma. The sample (3 mL of 10 mg/mL solution) was loaded onto a 20- × 3-cm column with a flow rate of 1 mL/min. The mobile phase was 10 mM phosphate buffer (pH 6.4) with a gradient of 0 to 1.0 M NaCl started 10 min after the sample addition. The column effluent was col-

lected in 5-mL aliquots and assayed for sugar content by the phenol-sulfuric acid assay as described below. Identified peaks were collected and screened for antigenicity by ELISA. A standard mixture of Glc and polygalacturonic acid (1 mg/mL) was used to calibrate the column.

### Dot-Blot Assay

Samples were solubilized in TBS (20 mM Tris and 0.5 M NaCl, pH 7.5) to 0.2 mg/mL, and 200 μL was added to each well of a dot-blot apparatus (Bio-Rad) and allowed to flow by gravity through the nitrocellulose membrane. Each well was washed with 200 μL of TBS and incubated with 200 μL of FGB-TBS for 1 h, followed by two washes with TBS. Hybridoma culture supernatant (200 μL; diluted 1:10 in TTBS [20 mM Tris, 0.5 M NaCl, 0.05% Tween 20, and 1% fish skin gelatin, pH 7.5]) was added and incubated for 1 h. The membranes were then removed and washed twice with TTBS for 5 min with gentle agitation, transferred to goat anti-mouse IgG, IgM, or polyvalent immunoglobulin labeled with horseradish peroxidase (diluted 1:1000 in TTBS), and incubated for 1 h with gentle agitation. Blots were then washed twice with TTBS and once with TBS as described above, developed in substrate solution (0.015 g of 4-chloro-1-naphthol in 5 mL of cold methanol added to 25 mL of TBS with 30 μL of 30% H<sub>2</sub>O<sub>2</sub>) for 1 h in the dark, and washed five times with double-distilled water. Blots were then imaged using a video camera (DXC-930 3-CCD, Sony, Tokyo, Japan) with output to a digitizer board (SNP-24, Active Imaging, Berkshire, UK). Image Tool version 1.25 (The University of Texas Health Science Center, San Antonio) was used to determine the density of bands with background subtraction of adjacent areas, providing averaged, background-subtracted values for each band. For each antibody, the background-subtracted value of *A. longipes* WIBS was designated as 100 and other values were scaled appropriately.

### Chemical Modification of *A. longipes* WIBS ECM

Periodate oxidation and 0.5 M NaOH treatment of *A. longipes* WIBS material were carried out according to Sledjeski and Weiner (1993). WIBS was desulfated by the methods of Falshaw and Furneaux (1994). The pyridinium salt was formed by dissolving 5 mg of purified WIBS in 1 mL of distilled water, passing the solution through a 5-mL column of Dowex 50W-X12 (H<sup>+</sup> form), adding excess pyridine, and freeze-drying.

Na<sub>2</sub>CO<sub>3</sub> and NaClO<sub>3</sub> treatments of *A. longipes* WIBS were done according to Fry (1988). All modified samples were assayed by dot-blot analysis, and NaOH-, Na<sub>2</sub>CO<sub>3</sub>-, and NaClO<sub>3</sub>-treated samples were also analyzed with size-exclusion chromatography to determine if the respective treatment reduced the size of the native polymers.

Uronosyl residues were converted to their corresponding neutral sugars (Taylor and Conrad, 1972) in a modified procedure as described below. *A. longipes* bicarbonate-soluble ECM (5 mg) was dissolved in 2 mL of 0.01 M NaAc (pH 4.75), CMC (0.5 mL of 250 mg CMC/mL of 0.01 M NaAc buffer, pH 4.75) was added, and the mixture was

stirred on ice for 2 h. Ice-cold 4 M imidazole HCl (0.5 mL), pH 7.0, was added, followed by 300 mg of NaB<sup>2</sup>H<sub>4</sub> powder, and stirred for 1 to 2 h (until effervescence ceased). The solution was then dialyzed against distilled water for 36 h, lyophilized, and assayed by dot-blot analysis as described previously.

*A. longipes* WIBS material was subjected to time-course hydrolysis by dissolving up to 5 mg/mL in 1 M TFA and incubating at 80°C for 30 min, 1 h, or 5 h. Samples were then dried under nitrogen in a 40°C water bath and assayed by dot-blot analysis, loaded onto a size-exclusion column as previously described, or derivatized for monosaccharide and linkage analysis.

Cleavage of *A. longipes* WIBS polysaccharides by lithium in ethylenediamine was carried out as described by Mort and Bauer (1982) with modifications as described by Lau et al. (1987). Reducing sugar assay and size-exclusion chromatography were used to verify polymer cleavage, and the samples were assayed by dot-blot analysis.

### Monosaccharide and Linkage/Substitution-Site Determination

Monosaccharide composition and linkage/substitution sites were determined by GC-MS of alditol acetates and partially methylated alditol acetates, respectively, as described previously (Wustman et al., 1997, and refs. therein). Samples were routinely hydrolyzed for 3 h at 121°C in 2 M TFA. Per-*O*-methylated alditol acetate mole percentages were calculated using effective carbon-response factors, as described by Sweet et al. (1975).

### Colorimetric Assays

Total carbohydrate and reducing sugar content were estimated by the phenol-sulfuric acid assay (Dubois et al., 1956) and the 3,5-dinitrosalicylic acid reagent assay (Miller, 1959), respectively, using a Gal:Fuc (1:1) standard curve.

## RESULTS

### Production of Hybridomas

Four hybridoma colonies producing antibodies with a high affinity for *A. longipes* WIBS material were cloned, and two other colonies producing only one class of antibody each were extended for possible future cloning. All hybridomas produced antibodies with  $\kappa$  light chains. Monoclonal antibodies AL.C1 and AL.C2 and uncloned hybridoma AL.E2 produced IgG1s, AL.C3 produced an IgG3, and AL.E1 produced IgMs.

### Cell Staining

FITC-conjugated anti-*A. longipes* antibodies differentially labeled *A. longipes* extracellular adhesives. The localization patterns for each antibody are summarized in Table I. All of the antibodies demonstrated the same specific labeling patterns of live cells, with similar titer, when PBS was replaced with seawater. AL.C1 and AL.E1 localized muci-

lage located between stacked cells and pads, collars, and portions of the shaft. AL.E1 labeling was most intense in the outer perimeter and central ribbon of the shaft core (Fig. 1B). AL.C1 uniformly labeled the shaft core (Fig. 1C), with a lower affinity for the outer layers, and also labeled material within the raphe (Fig. 1D), mucilage in the form of rings surrounding the terminal nodules, and amorphous mucilage associated with the cells and stalks. AL.C2, AL.C4, and AL.E2 (Fig. 1E) exhibited identical labeling patterns of shafts, pads, and collars, with binding restricted to the outermost layer of the shaft (Table I). AL.C3 labeled mucilage between cells (Table I) and amorphous mucilage loosely associated with the shafts (Table I; Fig. 1F) and frustules. Controls revealed no nonspecific antibody interactions (Fig. 1, G and H).

### Characteristics of Antigen Epitopes

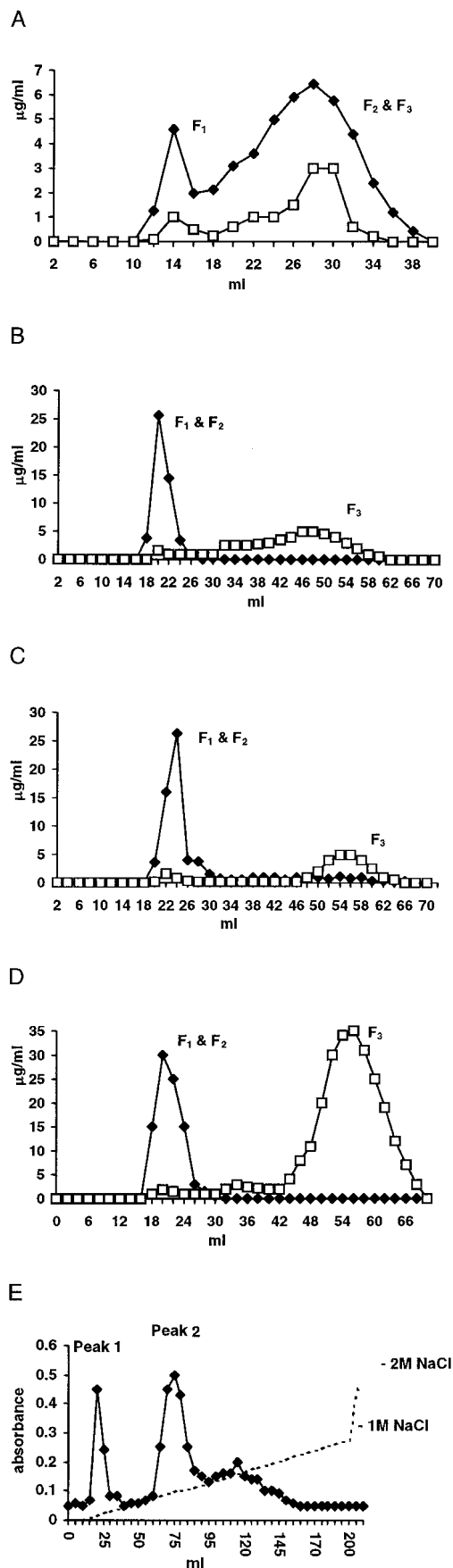
*A. longipes* WIBS material was separated into three size ranges by Sepharose 2B and Sephadex G-100 size-exclusion chromatography (Fig. 2, A and B): F<sub>1</sub>,  $\geq 20,000,000 M_r$ ; F<sub>2</sub>,  $\cong 100,000 M_r$ ; and F<sub>3</sub>,  $< 10,000 M_r$ , relative to dextran standards. F<sub>1</sub> and F<sub>2</sub> were the major fractions and consisted mostly of carbohydrate with a small amount of protein (F<sub>1</sub> approximately 5%, F<sub>2</sub> < 1%), whereas F<sub>3</sub> was almost entirely protein. F<sub>3</sub> produced a smear when separated by SDS-PAGE, indicating that carbohydrate was most likely still associated with the protein. WIBS material treated with 0.5 M NaOH (100 or 5°C) or trypsin and separated by size-exclusion chromatography yielded a decrease in F<sub>1</sub> and an increase in F<sub>2</sub>. F<sub>3</sub> yield also increased after the cold NaOH treatment, whereas trypsin degraded this fraction. Treatment with cold 0.5 M Na<sub>2</sub>CO<sub>3</sub> or 0.6 M NaClO<sub>3</sub> had no effect on the relative amounts of each fraction, indicating a lack of modification by cleavage of ester bonds or isodityrosine cross-links.

Size-exclusion chromatography of WIBS/CPC-soluble material also revealed F<sub>1</sub>, F<sub>2</sub>, and F<sub>3</sub> in similar proportions (Fig. 2C) to those shown for WIBS. However, if the imidazole buffer concentration was increased to 0.5 M, F<sub>3</sub> became the dominant fraction (Fig. 2D). This indicated that CPC

**Table I.** Summary of antibody localization patterns of *A. longipes* extracellular adhesive structures and affinities for highly sulfated and low-sulfate FGGs separated by anion-exchange column chromatography

Antibodies were detected by secondary anti-mouse polyvalent IgG, IgM and IgA conjugated with FITC. -, Affinity below detectable limits; +/-, low affinity; +, high affinity; and ++, very high affinity.

Adhesive Structure/Polymer	Antibodies					
	AL.C1	AL.C2	AL.C3	AL.C4	AL.E1	AL.E2
Shaft outer layers	-	+	-	+	+	+
Shaft core	+	-	-	-	-	-
Central ribbon	-	-	-	-	+	-
Pad and collar	+	+	+	+	+	+
Between cells	+	-	+	-	+	-
Highly sulfated FGG	++	+	+/-	+	+	+
Low-sulfate FGG	+	++	+/-	++	++	++



precipitation concentrates  $F_3$  (in the soluble fraction), although  $F_1$  and  $F_2$  are not completely removed (Fig. 2, C and D). If distilled water was used in place of imidazole HCl as the mobile phase, no fractionation occurred. WIBS/CPC-soluble material contained 5% more Man and 11% less Gal than the WIBS/CPC-insoluble fraction (Wustman et al., 1997), and methylation analysis disclosed a large decrease in the relative abundance of 2,3-Gal and 3,6-Gal, and an increase in t-Man and 4-Man residues. All antibodies except AL.C3 showed a high affinity for  $F_1$  and  $F_2$  and a reduced affinity for  $F_3$  (Table II). AL.C3 had a much lower affinity for WIBS than the other five antibodies, although antibody-FITC cell staining revealed that AL.C3 had a high affinity for the pads, collars, globular matrices associated with stalks and cells, and mucilage between stacked cells.

Anion-exchange chromatography separated WIBS into two fractions (Fig. 2E). Peak 1 eluted with the void volume and peak 2 eluted at approximately 0.3 M NaCl. Based on colorimetric assays, peak 1 was approximately 80% carbohydrate, 7% protein, 11% sulfate, and 18% uronic acid, and peak 2 was approximately 84% carbohydrate, 10% protein, 2% sulfate, and 19% uronic acid. IR analysis revealed absorbance at  $1240\text{ cm}^{-1}$  corresponding to sulfate ester (Craigie and Leigh, 1978) for both fractions. This absorbance was significantly reduced for peak 2, providing additional evidence of reduced sulfate content. Linkage/substitution-site profiles for peaks 1 and 2 were indistinguishable from those reported for WIBS material (Wustman et al., 1997).

Treatment of WIBS with 0.5 M NaOH (100 or  $5^\circ\text{C}$ ), trypsin (24 h), 0.5 M  $\text{Na}_2\text{CO}_3$ , and acidified  $\text{NaClO}_3$  had no effect on antigenicity, whereas CMC-activated reduction of uronosyl residues to the corresponding neutral sugars greatly increased affinity of all six antibodies relative to unmodified WIBS (Table II). Cleavage with lithium at the sites of uronic acids in ethylenediamine decreased antigenicity for AL.C1, AL.E1, and AL.E2, whereas periodate oxidation greatly decreased antigenicity for AL.C3 and AL.E1 and slightly decreased it for AL.C2 and AL.E2 (Table II). Desulfation of WIBS decreased antigenicity for AL.C4 (Table II). The affinity of five antibodies was greatly reduced after 1 M TFA hydrolysis (30 min at  $80^\circ\text{C}$ ) of WIBS and decreased below detection limits after hydrolysis for 5 h (Table II). Neutral-sugar analysis revealed that only Fuc was released after 30 min of 1 M TFA hydrolysis (30 min at  $80^\circ\text{C}$ ) and that Gal and Xyl were released after 1 and 5 h (Fig. 3). Linkage/substitution-site profiles of 30-min, 1-h,

**Figure 2.** Size-exclusion and anion-exchange chromatography of *A. longipes* WIBS extracellular adhesives. A, Sepharose 2B column chromatography of WIBS (mobile phase = 0.1 M imidazole HCl). B, Sephadex G-100 column chromatography of WIBS material (mobile phase = 0.1 M imidazole HCl). C, Sephadex G-100 column chromatography of WIBS/CPC-soluble material (mobile phase = 0.1 M imidazole HCl). D, Sephadex G-100 column chromatography of WIBS/CPC-soluble material (mobile phase = 0.5 M imidazole HCl). E, DEAE-Sephacel column chromatography of WIBS (mobile phase = 10 mM phosphate buffer).  $F_1$ , Polymers  $\geq 20,000,000\text{ M}_r$ ;  $F_2$ , polymers  $\approx 100,000\text{ M}_r$ ;  $F_3$ , polymers  $< 10,000\text{ M}_r$  relative to dextran standards.  $\blacklozenge$ , Carbohydrate;  $\square$ , protein; and dotted line, NaCl.

**Table II.** Interaction of antibodies with WIBS and fractions or modifications

*A. longipes* WIBS and chemically modified WIBS were blotted onto nitrocellulose and screened against supernatant from four cloned (AL.C1–AL.C4) and two uncloned (AL.E1 and AL.E2) hybridoma colonies. *A. coffeaeformis* WIBS was also blotted and screened against the antibodies for cross-reactivity. Detection was by peroxidase secondary anti-mouse antibody with digital imaging of the developed blot. Numbers represent averaged, background-subtracted density values that have been scaled to WIBS.

Isolated/Modified Fractions	AL.C1	AL.C2	AL.C3	AL.C4	AL.E1	AL.E2
	%					
<i>A. longipes</i> WIBS	100	100	100	100	100	100
<i>A. longipes</i> WIBS size-exclusion fractions						
F <sub>1</sub>	125	101	100	100	104	122
F <sub>2</sub>	66	100	150	95	113	111
F <sub>3</sub>	50	40	131	63	43	70
Modified <i>A. longipes</i> WIBS						
Desulfated	140	100	100	50	195	260
-COOH reduction	560	460	833	483	355	720
Uronic acid site cleavage	91	60	191	131	68	58
Periodate oxidation <sup>a</sup>	109	68	18	77	16	78
Sodium acetate buffer <sup>b</sup>	77	104	109	177	174	124
Hydrolyzed <i>A. longipes</i> WIBS						
1 M TFA (80°C), 30 min	50	20	73	31	42	22
1 M TFA (80°C), 1 h	0	0	18	0	16	3
1 M TFA (80°C), 5 h	0	0	0	0	3	0
<i>A. coffeaeformis</i> WIBS	53	9	0	7	12	0

<sup>a</sup> Periodate oxidation was carried out in 50 mM sodium acetate buffer, pH 4.5. <sup>b</sup> Treatment with 50 mM sodium acetate (pH 4.5) served as a control to rule out loss of antigenicity by periodate oxidation as a result of exposure to low pH.

and 5-h 1 M TFA hydrolysates compared with WIBS revealed that t-Fuc and 3-Fuc were released after 30 min of hydrolysis, as was the case after hydrolysis for 1 and 5 h (Table III). 2,3-Gal content significantly decreased after 1 h, whereas the molar percentage of 3- and 4-Gal dramatically increased with increasing hydrolysis times, and 2-Rha increased only after 5 h of hydrolysis (Table III). TLC revealed small oligosaccharides containing Fuc, Gal, and Xyl (5:1:1) released after 5 h of hydrolysis. Resistant material after 5 h of hydrolysis was mostly Gal with a small amount of Xyl and a trace amount of Fuc.

The antibodies were also screened by dot-blot analysis for cross-reactivity with *A. coffeaeformis* WIBS ECM. AL.C1 showed significant affinity for the *A. coffeaeformis* WIBS

material, whereas AL.C2, AL.C4, and AL.E1 exhibited a low level of cross-reactivity. Screening of the diatoms *C. cistula* and *S. decipiens* and associated ECM by antibody-FITC cell staining revealed no cross-reactivity for either diatom. Controls with nonimmune serum revealed no non-specific antibody interactions within the detection limits of the dot-blot immunoassay.

## DISCUSSION

Daniel et al. (1987) and Wang et al. (1997) demonstrated that the shafts of *A. longipes* consist of several outer layers oriented parallel to the axis of shaft elongation, and a core that has fibrous material organized in layered radial arrays perpendicular to the axis of shaft elongation and with a central ribbon. The uniqueness of these regions is supported by the successful generation of antibodies with differing affinities for each region. The six antibodies can be divided into three categories (Table I; Fig. 1) based on differing affinities for (a) regions other than the shaft, including pads, collars, and amorphous material loosely associated with the cells; (b) the outermost layers of the shaft; and (c) the central core. From these results it can be assumed that the antibodies recognize different epitopes that are distributed nonuniformly throughout the ECM. Spatial organization and induced conformational changes of antigenic molecules during the extracellular adhesive assembly process may account for the multiple localization patterns observed. Because all six antibodies showed a high affinity for *A. longipes* WIBS ECM, we fractionated WIBS by anion-exchange chromatography, size-exclusion chromatography, and CPC precipitation, and screened fractions for antigenicity.

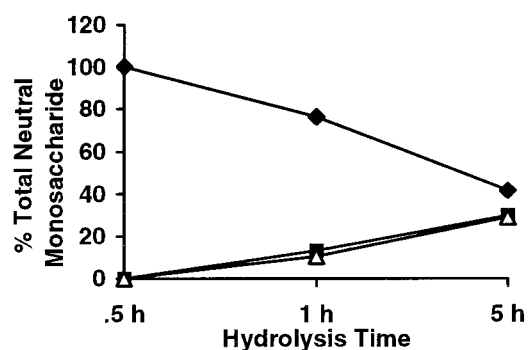


**Figure 3.** Monosaccharides released from *A. longipes* WIBS ECM by time-course hydrolysis (1 M TFA at 80°C). Fuc was the only neutral monosaccharide detected after 0.5 h of hydrolysis. Increasing amounts of Gal and Xyl were released after 1 and 5 h of hydrolysis. Neutral monosaccharide composition was determined by GC-MS of alditol acetates and is presented as a percentage of the total detected. ◆, Fuc; ■, Xyl; △, Gal.

**Table III.** Linkage/substitution-site profiles for *A. longipes* WIBS after time-course hydrolysis with 1 M TFA (80°C)

Glycosyl linkage/substitution sites of acid-resistant material were determined by GC-MS of partially methylated alditol acetates. Uronosyl residues were not determined. ND, Not detected.

Residue	0 h	0.5 h	1 h	5 h
	<i>mol%</i>			
Fucosyl				
t-Fuc	22	9.6	3.7	4
3-Fuc	20	7.5	4.8	1.2
4-Fuc	5.2	2.4	2.9	ND
2-Fuc	3	2.4	1.9	1.5
2,3-Fuc	2.2	1.6	1.7	0.4
3,4-Fuc	2	2.8	3.1	ND
2,4-Fuc	1.6	0.6	0.7	0.4
Rhamnosyl				
2-Rha	2.4	5.1	4.3	13.1
2,3-Rha	2	2.8	3.1	3.5
2,4-Rha	ND	1.1	1.9	1.7
Galactosyl				
2,3-Gal	11.1	10.2	3.5	4.8
3-Gal	4.6	10.8	14.7	14.7
3,6-Gal	1.7	5.8	7.7	5.3
4,6-Gal	1.7	5.4	6.8	7.3
t-Gal	1.1	1.8	2.4	2.6
6-Gal	0.8	3.5	4.3	4.1
4-Gal	0.8	7.7	9.5	12.1
Mannosyl				
t-Man	3.4	4.1	4.9	4.9
6-Man	1	2.4	2.3	2.1
2,4-Man	0.8	1.7	2.6	2.2
4-Gulosyl	0.5	3.8	3.6	5.1
Xylosyl				
t-Xyl	10.1	5.6	7.7	7
3-Xyl	2.1	1.5	2	2.2

### High- and Low-Sulfate FGGs

Using anion-exchange chromatography, we separated WIBS into two major fractions. Both fractions contained FGGs distinguishable from each other only by their sulfate content. Cell staining revealed that the antibodies with the highest affinity for the outer layers of the shaft (AL.C2, AL.C4, AL.E1, and AL.E2) also had a higher affinity for low-sulfate (2%) FGGs, whereas AL.C1 preferred the shaft core and had a higher affinity for high-sulfate (11%) FGGs. These results are in agreement with those of Johnson (1995) and Daniel et al. (1987). Johnson (1995) used x-ray microanalysis of sectioned *A. longipes* stalks to show that sulfate was located mainly in the stalk core, excluding the central ribbon, and Daniel et al. (1987) provided cytochemical evidence for a higher concentration of less-sulfated carboxylated polymers in the pads, collars, and outer layers of the shafts. Chemical and immunocytochemical evidence has now revealed that although these regions differ in polymer organization, they consist of related polymers (FGGs) that vary in their sulfate content. We hope to use this model system to investigate how such modifications affect polymer interactions, organization, and overall physical characteristics.

### Relationship of Shaft Polymers to Those Involved in Cell Motility

In addition to labeling the shaft core, AL.C1 also labeled the raphe region of motile *A. longipes* cells (Fig. 1D), demonstrating that the same epitope is present in stalks and material exuded from the raphe during cell motility. We have observed that the orientation of the shaft central ribbon always coincides with that of the raphe. However, differential antibody labeling indicates that the same epitopes are not available on this less-sulfated central-ribbon region as on the surrounding highly sulfated core. Evidence of a close relationship between polymers in the shaft central core and those raphe-derived materials involved in cell motility can be also found in lectin-labeling studies of Wustman et al. (1997), in which labeling by Fuc-binding lectin in the raphe correlated with periods of cell motility. This Fuc-binding lectin also labeled the stalk shaft cores. The importance of polysaccharide synthesis in stalk synthesis and cell motility is further indicated by the inhibition of both processes by the specific extracellular polysaccharide synthesis inhibitor dichlorobenzonitrile and related compounds (Wang et al., 1997). We conclude that the central core region of the shaft is raphe derived and is related to material exuded from the raphe during cell motility.

### Cross-Linking Proteins/Glycoproteins

Size-exclusion chromatography separated WIBS into three fractions: (a)  $F_1$ ,  $\geq 20,000,000 M_r$ ; (b)  $F_2$ ,  $\cong 100,000 M_r$ ; and (c)  $F_3$ ,  $< 10,000 M_r$  (Fig. 2).  $F_1$  and  $F_2$  appeared to be mostly carbohydrate and their monosaccharide profiles were indistinguishable, whereas  $F_3$  contained mainly protein/glycoprotein. The  $F_3$  fraction could be concentrated by precipitating out CPC-insoluble material. Monosaccharide profiles of the resulting CPC-soluble material revealed an increase in mannosyl residues (Wustman et al., 1997). The  $F_3$  fraction is water insoluble and can be separated from  $F_1$  and  $F_2$  only with relatively high concentrations of imidazole buffer. A plausible explanation for this may be that  $F_3$  contains mannoproteins that have a high affinity for other adhesive components found in  $F_1$  and  $F_2$ . Mannoproteins of *Candida albicans* fungal cell walls are involved in both covalent and noncovalent interactions, and have been shown to self-assemble in vitro after removal of the solubilizing agents by dialysis against double-distilled water (Sentandreu et al., 1995). Imidazole may prevent aggregation of polymers by interrupting ionic interactions. It has been shown that high concentrations of imidazole (0.5 M) can be used in place of *trans*-1,2-diaminocyclohexane-*N,N,N',N'*-tetraacetic acid and EDTA to solubilize pectins, presumably by competing with carboxyl groups for  $Ca^{2+}$  and thereby disrupting the "egg-box" formations (Mort et al., 1991). However, because neither chelating agents nor imidazole buffers solubilized intact *A. longipes* stalks, it appears that  $F_3$  protein does not cross-link native stalks via ionic interactions.

These proteins/glycoproteins appear to be involved in covalently linking the FGGs together, since treatments with

cold NaOH degraded  $F_1$ , releasing  $F_2$  and  $F_3$  polymers. Cold alkali treatments are fairly specific for cleavage of *O*-glycosidic linkages of sugar proteins/glycoproteins in ECM (Fry, 1988), and such cross-linking components may be present in the  $F_3$  fraction.  $F_1$  was also converted to  $F_2$  by treatment with trypsin, providing further evidence for the cross-linking of  $F_2$  polymers by proteins/glycoproteins into large  $F_1$  complexes. Because  $\text{NaClO}_2$  and cold  $\text{Na}_2\text{CO}_3$  treatments did not degrade  $F_1$ , ester-linked phenolics or isodityrosine linkages are most likely not important in bridging the  $F_2$  molecules. Because trypsin and NaOH treatments of WIBS did not affect antigenicity, it appears that all of the antibodies recognized carbohydrate epitopes of the FGGs or of a possible glycoprotein described above. It is also possible that such glycoproteins from *A. longipes* play a more direct role in adhesion and motility. In the marine diatom *S. decipiens*, antibodies raised against extracellular proteoglycans localized material associated with the raphe and inhibited both cell motility and adhesion (Lind et al., 1997).

### Characterization of the Antibody Epitopes

Wustman et al. (1997) identified t-Fuc residues throughout the entire stalk and between stacked cells preparing to separate. It was found that Fuc made up 42% of the WIBS ECM, one-half of which was t-Fuc residues, as estimated by linkage analysis (Wustman et al., 1997). Thus, it would be reasonable to assume that these residues may be important in inducing antibody formation because so many t-Fuc residues are available, and terminal nonreducing sugars are commonly recognized as the immunodominant group of branched polysaccharides (Kabat, 1976). This may be why some of the antibodies showed a small amount of cross-reactivity with *A. coffeaeformis* WIBS ECM, which also contains a substantial amount of t-Fuc (Wustman et al., 1997). *C. cistula*, which contains mostly Gal and Xyl and lacks Fuc (Wustman et al., 1997), showed no detectable cross-reactivity.

The importance of fucosyl residues in antibody-antigen recognition was further demonstrated by a time-course hydrolysis with TFA. Antigenicity was significantly reduced for five antibodies after 30 min of 1 M TFA hydrolysis (80°C). The exception was AL.C3, which retained more than 70% of its original interaction with WIBS. Linkage/substitution analysis of the 30-min 1 M TFA-resistant material revealed a major decrease in t-Fuc and 3-Fuc residues, and monosaccharide analysis revealed that only fucosyl monomers were released after 30 min of TFA hydrolysis. 3-Fuc and t-Fuc may make up short 2-unit side chains or the ends of longer side chains, since 3-Fuc and t-Fuc residues are estimated by linkage/substitution analysis to be present in a ratio of  $\approx 1:1$  (Table III). Loss of antigenicity by removal of ester sulfate during hydrolysis can be ruled out for all of the antibodies except AL.C4, for which desulfation of WIBS reduced antigenicity by 50% (Table II). However, because antigenicity was not completely lost after desulfation, but was below detection limits after 1 h of TFA hydrolysis, it would seem that TFA hydrolysis does not affect AL.C4 affinity for WIBS by de-

sulfation alone. Because removal of fucosyl residues greatly reduced antigenicity in comparison with desulfation, NaOH and trypsin treatments, CMC-activated reduction, and polymer cleavage by lithium at uronic acid sites in ethylenediamine, five antibodies appeared to recognize fucosyl-containing side chains, regions near these side chains, or regions that depend on these side chains to maintain conformation of the epitope. Furthermore, antigenicity for WIBS was significantly reduced by periodate oxidation for AL.C2, AL.E1, and AL.E2, as would be expected if t-Fuc units played a role in antibody-antigen recognition. Fucosyl-containing side chains are most likely responsible for the hydrophobic nature of the stalks (Wang et al., 1997; Wustman et al., 1997) involved in initial passive attachment (Wang et al., 1997), and further studies with the antibodies characterized here may help to understand how these side chains interact and contribute to such overall characteristics as flexibility, tensile strength, resistance to microbial degradation, and cell adhesion.

AL.C3 had a unique labeling pattern in that it bound only to pads/collars and "amorphous" material but did not bind to shafts. Although bacteria are often associated with this amorphous material, AL.C3 did not localize individual bacteria. The material appears to be diatom derived, as shown by time-lapse microscopy, which revealed material that escaped from between the girdle bands, expanded rapidly, and remained loosely associated with the cells and stalks (data not shown). AL.C3 was the only antibody to show a higher affinity to  $F_3$  than to WIBS, and the epitope was much more resistant to partial acid hydrolysis than to the other antibodies. These results indicate a common epitope in the amorphous material of pads/collars, the globular matrix materials surrounding cells, and in the  $F_3$  protein that cross-links shaft polymers. The Man content of this  $F_3$  fraction may account for the many previous reports of Man in extracellular polymeric substances closely associated with diatom frustules (Hoagland et al., 1993).

### Adhesive Model and Conclusions

Anion-exchange and size-exclusion column chromatography revealed highly sulfated (11%) and low-sulfate (2%) FGGs of  $\approx 100,000 M_r$  (relative to dextran). Five of the antibodies raised against *A. longipes* adhesive structures appear to recognize a family of related epitopes with antigenicity dependent on fucosyl-containing side chains present on both the highly sulfated and the low-sulfate FGGs. These polysaccharides are cross-linked via *O*-glycosidic sugar-protein linkages into large ( $>20,000,000 M_r$ ) proteoglycan assemblages. The antibody AL.C1, which localized the shaft core, had a higher affinity for the highly sulfated FGGs, and the antibodies AL.C2, AL.C4, AL.E1, and AL.E2, which localized the outer layers of the shaft, had higher affinities for the low-sulfate FGGs. AL.C3 appears to recognize a unique epitope in pads, collars, globular material surrounding and between cells, and in the  $F_3$  protein fraction.

Based on these results, we present an adhesive model summarized in Figure 4. This model predicts that a hollow cylinder made up of polymers oriented parallel to the

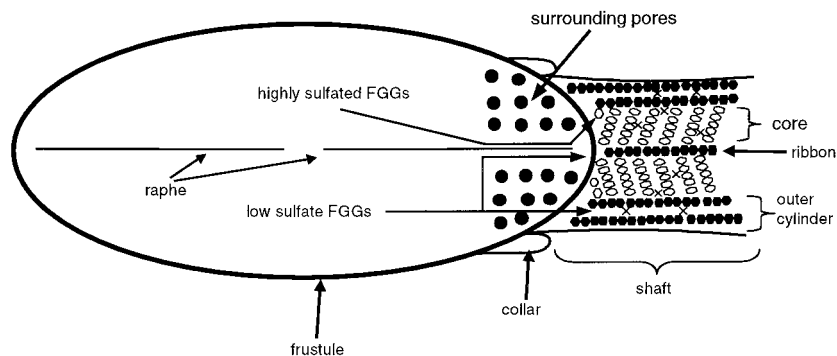


**Figure 4.** Model of the stalk of *A. longipes* detailing the location of components characterized here and putative sites of origin from the frustule. A hollow cylinder made up of polymers oriented parallel to the length of the stalk is created when low-sulfate FGGs are expelled through pores surrounding the terminal region of the raphe. Simultaneously, highly sulfated FGGs are expelled through the raphe terminus, expanding into the hollow cylinder and forming a fibrillar array of polymers oriented perpendicular to the length of the shaft. The FGGs are then cross-linked extracellularly by protein and phenolic components. ×, Protein or phenolic cross-link; ○, highly sulfated FGG; and ●, low-sulfate FGG.

length of the stalk is created when low-sulfate FGGs are expelled through pores surrounding the terminal region of the raphe. Highly sulfated FGGs are expelled through the raphe terminus, expanding into the hollow cylinder, forming a fibrillar array of polymers oriented perpendicular to the length of the shaft. Antibody localization results indicate that this central core region of the shaft is related to material exuded from the raphe during cell motility. Cross-linking of FGGs by protein and phenolic components serves to cure the adhesive structure. Future testing of this model and work with these antibodies will help to improve our understanding of adhesive architecture and the inter- and intramolecular interactions responsible for the overall characteristics of extracellular adhesives generated by diatoms.

#### ACKNOWLEDGMENTS

The authors thank Tony Chiovitti and Yan Wang for helpful comments and discussions.

Received September 19, 1997; accepted December 19, 1997.  
Copyright Clearance Center: 0032-0889/98/116/1431/11.

#### LITERATURE CITED

- Craigie JS, Leigh C** (1978) Carrageenans and agars. In JA Hellebust, JS Craigie, eds, *Handbook of Phycological Methods: Physiological and Biochemical Methods*. Cambridge University Press, Cambridge, UK, pp 109–131
- Daniel GF, Chamberlain AHL, Jones EBG** (1987) Cytochemical and electron microscopical observations on the adhesive materials of marine fouling diatoms. *Br Phycol J* **22**: 101–118
- Dubois M, Gilles KA, Hamilton JK, Rebers PA, Smith F** (1956) Colorimetric method for determination of sugars and related substances. *Anal Chem* **28**: 350–356
- Falshaw R, Furneaux RH** (1994) Carrageenan from the tetrasporic stage of *Gigartina decipiens* (Gigartinales, Rhodophyta). *Carbohydr Res* **252**: 171–182
- Freshour G, Clay RP, Fuller MS, Albersheim P, Darvill AG, Hahn MG** (1996) Developmental and tissue-specific structural alterations of the cell-wall polysaccharides of *Arabidopsis thaliana* roots. *Plant Physiol* **110**: 1413–1429
- Fry SC** (1988) *The Growing Plant Cell Wall: Chemical and Metabolic Analysis*. John Wiley & Sons, New York
- Harlow E, Lane D** (1988) *Antibodies: A Laboratory Manual*. Cold Spring Harbor Laboratory Press, Cold Spring Harbor, NY
- Hoagland KD, Rosowski JR, Gretz MR, Roemer SC** (1993) Diatom extracellular polymeric substances: function, fine structure, chemistry, and physiology. *J Phycol* **29**: 537–566
- Johnson LM** (1995) *Physiology of *Achnanthes longipes* Ag.: nutritional requirements for the secretion of extracellular polymer substances*. PhD thesis. University of Nebraska, Lincoln
- Kabat EA** (1976) *Structural Concepts in Immunology and Immunochimistry*. Holt, Rinehart and Winston, New York
- Lau JM, McNeil M, Darvill AG, Albersheim P** (1987) Selective degradation of the glycosyluronic acid residues of complex carbohydrates by lithium dissolved in ethylenediamine. *Carbohydr Res* **168**: 219–243
- Levy S, Staehelin LA** (1992) Synthesis, assembly and function of plant cell wall macromolecules. *Current Opinion in Cell Biology* **4**: 856–862
- Lind JL, Heimann K, Miller EA, van Vliet C, Hoogenraad NJ, Wetherbee R** (1997) Substratum adhesion and gliding in a diatom are mediated by extracellular proteoglycans. *Planta* **203**: 213–221
- McCann MC, Wells B, Roberts K** (1990) Direct visualization of cross-links in the primary plant cell wall. *J Cell Sci* **96**: 323–334
- Miller GL** (1959) Use of dinitrosalicylic acid reagent for determination of reducing sugars. *Anal Chem* **31**: 426–428
- Mort AJ, Bauer WD** (1982) Application of two new methods for cleavage of polysaccharides into specific oligosaccharide fragments. *J Biol Chem* **257**: 1870–1875
- Mort AJ, Moerschbacher BM, Pierce ML, Maness NO** (1991) Problems encountered during the extraction, purification, and chromatography of pectic fragments, and some solutions to them. *Carbohydr Res* **215**: 219–227
- Penel C, Greppin H** (1996) Pectin binding proteins: characterization of the binding and comparison with heparin. *Plant Physiol Biochem* **34**: 479–488
- Puhlmann J, Bucheli E, Swain MJ, Dunning N, Albersheim P, Darvill AG, Hahn MG** (1994) Generation of monoclonal antibodies against plant cell-wall polysaccharides. I. Characterization of a monoclonal antibody to a terminal alpha-(1→2)-linked fucosyl-containing epitope. *Plant Physiol* **104**: 699–710
- Sentandreu R, Sentandreu M, Elorza MV, Iranzo M, Mormeneo S** (1995) Interactions of proteins with other wall components: a pivotal step in fungal cell wall construction. *Can J Bot* **73**: S384–S387
- Sledjeski DD, Weiner RM** (1993) Production and characterization of monoclonal antibodies specific for *Shewanella colwelliana* exopolysaccharide. *Appl Environ Microbiol* **59**: 1565–1572
- Sweet DP, Shapiro RH, Albersheim P** (1975) Quantitative analy-

- sis by various g.l.c. response-factor theories for partially methylated and partially ethylated alditol acetates. *Carbohydr Res* **40**: 217–225
- Taylor JG, Haigler CH** (1993) Patterned secondary cell-wall assembly in tracheary elements occurs in a self-perpetuating cascade. *Acta Bot Neerl* **42**: 153–163
- Taylor RL, Conrad HE** (1972) Stoichiometric depolymerization of polyuronides and glycosaminoglycuronans to monosaccharides following reduction of their carbodiimide-activated carboxyl groups. *Biochemistry* **11**: 1383–1389
- Wang Y, Lu J-C, Mollet J-C, Gretz MR, Hoagland KD** (1997) Extracellular matrix assembly in diatoms (Bacillariophyceae). II. 2,6-Dichlorobenzonitrile inhibition of motility and stalk production in the marine diatom *Achnanthes longipes*. *Plant Physiol* **113**: 1071–1080
- Wustman BA, Gretz MR, Hoagland KD** (1997) Extracellular matrix assembly in diatoms (Bacillariophyceae). I. A model of adhesives based on chemical characterization and localization of polysaccharides from the marine diatom *Achnanthes longipes* and other diatoms. *Plant Physiol* **113**: 1059–1069